Title

Glioblastoma Recurrence and the Role of O6-Methylguanine—DNA Methyltransferase Promoter Methylation

Journal

JCO Clinical Cancer Informatics, 3(3)

ISSN

2473-4276

Authors

Storey, Katie
Leder, Kevin
Hawkins-Daarud, Andrea
et al.

Publication Date

2019-12-01

DOI

10.1200/cci.18.00062

Peer reviewed

SPECIAL SERIES: MATHEMATICAL ONCOLOGY

review article

Glioblastoma Recurrence and the Role of O^6-Methylguanine–DNA Methyltransferase Promoter Methylation

Katie Storey, PhD[1]; Kevin Leder, PhD[1]; Andrea Hawkins-Daarud, PhD[2]; Kristin Swanson, PhD[2]; Atique U. Ahmed, PhD[3]; Russell C. Rockne, PhD[4]; and Jasmine Foo, PhD[1]

abstract

Tumor recurrence in glioblastoma multiforme (GBM) is often attributed to acquired resistance to the standard chemotherapeutic agent, temozolomide (TMZ). Promoter methylation of the DNA repair gene MGMT (O^6-methylguanine–DNA methyltransferase) has been associated with sensitivity to TMZ, whereas increased expression of MGMT has been associated with TMZ resistance. Clinical studies have observed a downward shift in MGMT methylation percentage from primary to recurrent stage tumors; however, the evolutionary processes that drive this shift and more generally the emergence and growth of TMZ-resistant tumor subpopulations are still poorly understood. Here, we develop a mathematical model, parameterized using clinical and experimental data, to investigate the role of MGMT methylation in TMZ resistance during the standard treatment regimen for GBM—surgery, chemotherapy, and radiation. We first found that the observed downward shift in MGMT promoter methylation status between detection and recurrence cannot be explained solely by evolutionary selection. Next, our model suggests that TMZ has an inhibitory effect on maintenance methylation of MGMT after cell division. Finally, incorporating this inhibitory effect, we study the optimal number of TMZ doses per adjuvant cycle for patients with GBM with high and low levels of MGMT methylation at diagnosis.

INTRODUCTION

Glioblastoma multiforme (GBM) is an aggressive form of brain cancer with poor prognosis. Typically, patients with GBM are treated with surgical resection followed by radiation therapy and chemotherapy with the oral alkylating agent, temozolomide (TMZ). This standard regimen results in a median survival of only 15 months and a 2-year survival rate of 30%.[1] The effectiveness of TMZ is affected by the methylation status of the promoter for DNA repair protein O^6-methylguanine–DNA methyltransferase (MGMT). Clinical studies have linked epigenetic silencing of *MGMT* via promoter methylation with greater sensitivity to TMZ and improved patient prognosis,[2,3] whereas resistance to TMZ has been associated with increased expression levels of MGMT.[2,4,5]

Studies have compared MGMT promoter methylation in newly diagnosed tumors with matched recurrence samples after TMZ treatment.[6-9] These studies provide evidence of a downward shift in the MGMT promoter methylation percentage during treatment. For example, in Brandes et al,[6] eight of 13 patients transitioned from an MGMT-methylated primary tumor to an unmethylated recurrent tumor after treatment, and in Suzuki et al,[7] it was reported that 10 of 13 patients switched from a methylated primary tumor to an unmethylated recurrent tumor. In Christmann et al,[9] the authors observed that 39.1% of pretreatment GBM and 5.3% of recurrences were promoter methylated in addition to an observed increase of MGMT activity in recurrences. In Jung et al,[8] 15 of 18 recurrence samples displayed higher MGMT expression than matched primary samples; however, it is unclear whether this transition from methylated to unmethylated recurrent tumors is a result of TMZ actively influencing the methylation status of MGMT, as some have hypothesized,[5,6,10] simply a result of evolutionary selection for a more drug-tolerant phenotype, or some combination of both processes. We strive to understand this question by modeling the evolutionary processes that drive this shift.

Previous works have mathematically modeled the response of glioblastoma to treatment. In Levin et al,[11] the authors model chemotherapeutic delivery to brain tumors using a two-compartment catenary model. In Stamatakos et al,[12] a spatiotemporal model that allows for TMZ optimization specific to patients with GBM is developed. The model in Böttcher et al[13] explores interactions between rapidly proliferating GBM cells

ASSOCIATED CONTENT

Data Supplement

Author affiliations and support information (if applicable) appear at the end of this article.

Accepted on October 23, 2018 and published at ascopubs.org/journal/cci on February 13, 2019: DOI https://doi.org/10.1200/CCI.18.00062

and a dormant cell population. The effect of fractionated radiation dosing on GBM is studied using the linear-quadratic (L-Q) model.[14-17] Powathil and colleagues[18] consider a spatiotemporal brain tumor model that includes effects from both radiotherapy and chemotherapy. Patient-specific models of glioblastoma are developed in Rockne et al[19] and Esteller et al[20] to predict patient response to radiotherapy and to determine optimal dosing strategies. Many more mathematical modeling efforts that focus on glioblastoma growth and therapy response are reviewed in Håvik et al.[21] Mathematical models have also been developed to describe the process of DNA methylation changes in cells.[22-26] For example, Otto and Walbot[23] introduced the first model that describes methylation in terms of maintenance and de novo methylation. A similar model in a continuous-time framework was developed in Pfeifer et al.[26] We consider a discrete-time Markov chain version of the methylation model by Otto and Walbot, presented by Sontag and colleagues.[25]

Here, we develop and parameterize a stochastic model of the evolutionary dynamics that drive GBM response to standard treatment. We incorporate a variant of the methylation model in Sontag et al[25] to investigate the role of MGMT promoter methylation in TMZ resistance. In particular, we focus on the specific roles of three major DNA methyltransferases—DNMT1, DNMT3a, and DNMT3b—within the methylation process, illustrated in Figure 1A. DNMT1 is responsible for maintenance methylation in which patterns of methylation in the original parental DNA are preserved in the replicated DNA. DNMT3a and DNMT3b are responsible for de novo methylation in which unmethylated sites in the parental DNA become methylated in the replicated DNA.[27-29] Of note, we focus on passive demethylation rather than active demethylation that results from ten-eleven translocation (TET) enzyme–mediated oxidation, as the precise mechanisms of active demethylation are still uncertain and several studies have suggested that hypoxylation of 5-methylcytosine by TET enzymes may result in demethylation by inhibiting DNMT1 activity.[30-33] Thus, rather than incorporating active methylation as an independent mechanism, we assume that the activity of TET1 and TET2 may implicitly affect the passive

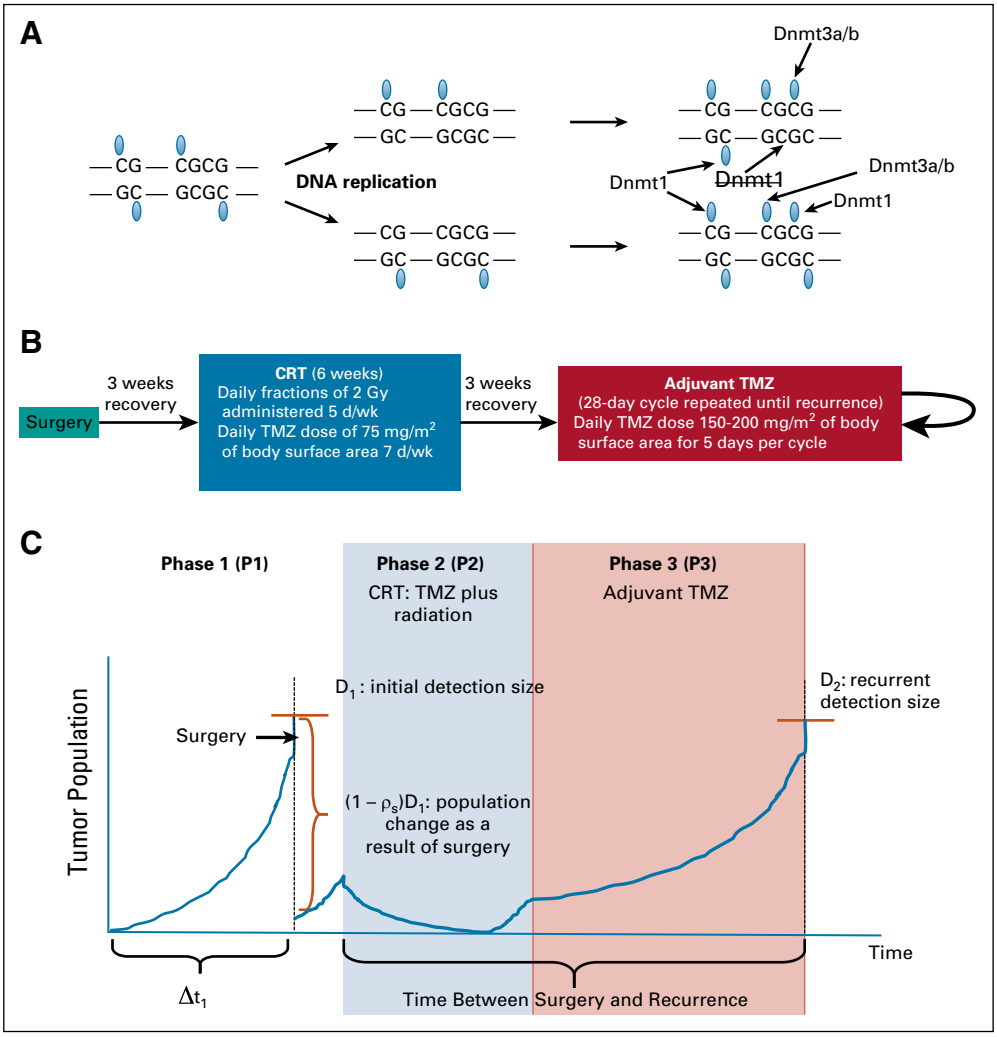

FIG 1. (A) Diagram illustrates a portion of a DNA molecule splitting during replication and the role of the DNA methyltransferases DNMT1 and DNMT3a/b. Notice that DNMT1 methylates the sites in the new strand that were methylated in the parental strand. As this process is not perfect, some sites can be missed. Dnmt3a/b methylates new sites that were not previously methylated in the top strands of the upper and lower molecules. This figure is similar to a figure in Sontag et al.[25] (B) Standard treatment schedule for GBM.[7] (C) The three phases (P) of the model. P1 consists of the tumor growth before detection and surgery, P2 denotes the concurrent radiation and chemotherapy (CRT) phase of treatment, and P3 refers to the adjuvant chemotherapy after CRT. TMZ, temozolomide.

methylation parameters within our model. By incorporating detailed mechanisms of maintenance and de novo methylation—driven by DNMT1, DNMT3a, and DNMT3b—within an evolutionary model of GBM treatment response, this work provides unique insight into the dynamics of MGMT methylation and GBM recurrence.

The outline of this paper is as follows: Mathematical Model describes the framework of the mathematical model, and Experimental and Clinical Data details the clinical and experimental data we collected and used to parameterize the model. In Results, we present our findings regarding methylation changes in tumors during therapy and optimal TMZ dosing strategies. We summarize these results and discuss future directions in Discussion.

MATHEMATICAL MODEL

We develop a stochastic model that describes the evolutionary dynamics of GBM response to standard treatment. We use a multitype, continuous-time birth-death process model (eg, see Athreya and Ney[34]) in which each cell waits an exponential amount of time before division or death as governed by its birth and death rates. The model consists of three GBM cellular subtypes: type 1, with fully methylated MGMT promoters; type 2, with hemimethylated MGMT promoters; and type 3, with unmethylated MGMT promoters. Type 1 cells are TMZ sensitive, and type 2 and type 3 cells are considered TMZ resistant because they both possess the ability to repair the lesion created by TMZ. Let $X_1(t)$, $X_2(t)$, and $X_3(t)$ denote the number of type 1, type 2, and type 3 cells, respectively, at time t. Cellular birth and death rates vary during treatment with TMZ and radiation and are estimated with experimental data (Data Supplement). TMZ-resistant cells, $X_2(t)$ and $X_3(t)$, are assumed to have the same birth and death rates.

Conversions also occur between cell types as driven by methylation/demethylation on the MGMT promoter immediately after cell division. To model these processes, we use a variant of the description in Sontag et al[25] to describe maintenance and de novo methylation at a CpG site. This underlying methylation model feeds into our population-level branching process model via rates of conversion between cellular subtypes. More specifically, let ρ be the probability of maintaining methylation for any given CpG site after replication—that is, the probability that DNMT1 methylates a CpG dyad after replication, conditioned on the event that the site was methylated before replication. Let ν be the probability of de novo methylation—that is, the probability that DNMT3a or DNMT3b methylates any CpG site that is unmethylated immediately after DNA replication. Inspired by Sontag et al,[25] we derived offspring distributions for each of the three cell types, conditioned on cell division. In these distributions, $p_i(x, y, z)$ refers to the probability that a type i cell will produce x type 1 cells, y type 2 cells, and z type 3 cells after replication. For ease of notation, let $A := (1-\rho)(1-\nu)$..

$$\begin{aligned} p_1((2,\,0,\,0)) &= (1-A)^2 \\ p_1((1,\,1,\,0)) &= 2A(1-A) \\ p_1((0,\,2,\,0)) &= A^2 \end{aligned} \tag{1}$$

$$\begin{aligned} p_2((2,\,0,\,0)) &= \nu^2(1-A) \\ p_2((1,\,1,\,0)) &= 2\nu(1-\nu)(1-A) + \nu^2 A \\ p_2((1,\,0,\,1)) &= (1-\nu)^2(1-A) \\ p_2((0,\,2,\,0)) &= 2\nu(1-\nu)A \\ p_2((0,\,1,\,1)) &= A(1-\nu)^2 \end{aligned} \tag{2}$$

$$\begin{aligned} p_3((2,\,0,\,0)) &= \nu^4 \\ p_3((1,\,1,\,0)) &= 4(\nu^3-\nu^4) \\ p_3((1,\,0,\,1)) &= 2\nu^2(1-\nu)^2 \\ p_3((0,\,2,\,0)) &= 4\nu^2(1-\nu)^2 \\ p_3((0,\,1,\,1)) &= 4\nu(1-\nu)^3 \\ p_3((0,\,0,\,2)) &= (1-\nu)^4 \end{aligned} \tag{3}$$

The Data Supplement depicts the set of possible birth events. Of note, a methylated dyad produces two hemimethylated dyads when the DNA strands split during replication, and those sites remain hemimethylated if the site without methylation is not methylated by DNMT1 or DNMT3a/b immediately after replication. Hence, the probability that each dyad remains hemimethylated is $A = (1-\rho)(1-\nu)$, and consequently the probability of producing two hemimethylated dyads—that is, two type 2 cells—is A^2. Conversely, the probability that one of those hemimethylated sites becomes fully methylated is $1-A$, so the probability of producing two fully methylated (type 1) cells is $(1-A)^2$, and the probability of producing one type 2 and one type 1 cell is $A(1-A)$. Offspring distributions for type 2 and type 3 cell replication can be verified similarly upon inspection using the idea that an unmethylated dyad produces two unmethylated dyads during replication and each CpG site within these dyads can only be methylated with DNMT3a/b—that is, via de novo methylation. Later, as we investigate the potential impact of TMZ on the methylation processes, we allow the de novo and maintenance probabilities to vary in the presence of TMZ.

The binary stratification of tumors into MGMT methylated or MGMT unmethylated in the clinical literature requires some clarification as methylation status can vary between tumor cells and between CpG sites in the same genic promoter region. Typically, the percentage of methylated cells is determined for a small subset of CpG sites in the MGMT promoter region and averaged across sites. Then a threshold, which may vary widely between studies, is used to stratify tumors into methylated versus unmethylated status. As a result of substantial variation between studies in

the definition of this threshold, here we model quantitative changes in methylation percentage on a representative CpG site rather than imposing a binary stratification.

The model describes three phases of tumor development and standard GBM treatment. Phase 1 consists of tumor growth before detection, surgery, and a 3-week recovery. Phase 2 consists of concurrent radiotherapy and chemotherapy for 6 weeks, followed by a 3-week recovery. During chemotherapy, daily radiation fractions of 2 Gy are administered 5 days per week and TMZ 75 mg per day is administered per square meter of body surface area. Phase 3 consists of repeated 28-day cycles of adjuvant chemotherapy—five daily doses of TMZ 150 to 200 mg/m^2, followed by a 23-day recovery—until tumor recurrence. Additional details are described in Stupp et al.[1] Schematics of the standard GBM treatment schedule and the three phases are provided in Figure 1. Below we describe the adaptation of the branching process dynamics during each phase.

Phase 1: Pretreatment, Surgery, and Recovery

In the absence of treatment, intrinsic birth rates of untreated methylated (type 1) and hemi-/unmethylated (type 2/type 3) cells are b_1 and b_2 per day, respectively, and their death rates are c_1 and c_2. The parameters of the model are determined using experimental and clinical data (Data Supplement), and a summary of the baseline parameter set is provided in the Data Supplement. The model starts with a single methylated cell, and once the tumor population reaches a detection size threshold D_1, we model surgical resection of the tumor by removing p_s percent of the total cells, chosen proportionally for each subtype. During the 3-week recovery period, the initial birth and death rates drive the regrowth of the tumor.

Phase 2: TMZ, Radiation for 6 Weeks, and Recovery

In phase 2, the tumor undergoes concurrent radiotherapy and chemotherapy for 6 weeks. The standard schedule for radiotherapy is a daily fraction of 2 Gy administered 5e days per week, Monday through Friday. In addition, the tumor is treated every day with TMZ 75 mg per square meter of body surface area. As TMZ is a cytotoxic treatment, we model its impact by increasing the death rates of the tumor cells, denoted c_1 and c_2. Let $g_1(t)$, $g_2(t)$ be the additional death rate as a result of TMZ treatment of type 1 and type 2/type 3 cells, respectively. These rates depend on the current TMZ concentration level and are determined from experimental and pharmacokinetic data, detailed in the Data Supplement.

The cytotoxic effect of radiotherapy is modeled using the standard L-Q L-model.[16] Here, radiosensitivity parameters α, β are used to account for toxic lesions to DNA and misrepair of repairable damage to DNA, respectively.[35] We chose to use the L-Q model because it is a parsimonious model that has shown good agreement with experiments. Whereas there are many important extensions to this model, here we use the standard version as the effects of radiation are not the main focus of this work. Under the standard L-Q model, the probability of cell survival at the time of each radiation dose d is $S(d) = exp(-\alpha d - \beta d^2)$. At the time t of each radiation dose, we remove $(1 - S(d))X_1(t)$ type 1 cells, $(1 - S(d))X_2(t)$ type 2 cells, and $(1 - S(d))X_3(t)$ type 3 cells, where $d = 2$ Gy for all doses during phase 2. During the 3-week recovery, cellular birth and death rates revert to those used in the pretreatment phase. Given data constraints, we ignore differences in radiosensitivity between type 1 and type 2/3 cells.

Phase 3: Adjuvant TMZ

During phase 3, adjuvant chemotherapy is administered to the tumor. In this phase, the additional death rates $g_1(t)$ and $g_2(t)$ as a result of chemotherapy reflect five daily TMZ doses of 150 to 200 mg/m^2, followed by 23 days off. This 28-day cycle repeats until tumor recurrence, which occurs when the tumor population size reaches the threshold D_2.

EXPERIMENTAL AND CLINICAL DATA

Experimental Setup

We performed experiments on patient-derived xenograft (PDX) cell lines to investigate the differential impact of TMZ on growth kinetics of MGMT-methylated and -unmethylated GBM cells. PDX glioma specimens (GBM6) were obtained from C. David James, MD, at Northwestern University and maintained according to published protocols.[5] Cells were propagated in vivo by injecting them into the flank of nu/nu athymic nude mice. In vitro experiments with these cells were performed using DMEM that was supplemented with 1% fetal bovine serum and 1% penicillin–streptomycin antibiotic mixture. All cells were maintained in a humidified atmosphere with CO_2 and temperature carefully kept at 5% and 37°C, respectively. We performed dissociations enzymatically using 0.05% trypsin and 2.21 mmol/L EDTA solution (Corning, Corning, NY, USA). The GBM6 PDX cell line contains an unmethylated MGMT promoter, evaluated by using a standard reverse transcription polymerase chain reaction assay. In brief, DNA was extracted from an orthotropic tumor using Qiagen DNA extraction kits (Qiagen, Wetzlar, Germany).[36] Isolated tumor DNA was bisulfite treated using the EZ DNA methylation kit (Zymo Research, Orange, CA). Modified DNA was amplified using primers specific for either methylated or unmethylated MGMT promoter sequences as described previously.[37] The clinically relevant regimen for TMZ consists of 150 to 200 mg/m^2 per day, administered orally, on days 1 to 5 of a 28-day cycle[1]; however, its peak concentration measured is only 50 μmol/L in a patient's blood samples[38-40] and 5 μmol/L in CSF.[40] Thus, it has been proposed that the intratumoral concentration may not exceed 50 μmol/L.[38] IC_{50} values for GBM cell lines and xenografted specimens used throughout our experiments

were significantly higher than the therapeutic concentrations of TMZ observed in patients (data not shown). On this basis, we chose to use TMZ 5 and 500 μmol/L throughout our experiments. After 8 days, all cells were euthanized at the maximum dose of 500 μmol/L; thus, this time window was used.

In these in vitro experiments, plates of 48,000 GBM6 cells were treated in triplicate at eight concentrations of TMZ, including in a control group that was treated with dimethyl sulfoxide. Live and dead cell counts were collected via MTT and trypan blue assays after 8 days of exposure. The average number of live cells for each TMZ concentration is shown in Figure 2A. Figure 2B plots the average proportion of live cells from the sum of live and dead cells after 8 days of exposure for various TMZ doses. The frequency of cells that express MGMT, as assessed in each group after 8 days, is shown in Figure 2C. These data are used in the Data Supplement to fit Hill equations that describe the percentage of viable type 1 and type 2/type 3 cells as a function of TMZ concentration.

To examine MGMT expression, during therapy TMZ-treated cells were collected at a designated time. Cells were then treated with fixation and permeabilization buffers (eBioscience, San Diego, CA, USA) according to the manufacturer's instructions. After fixation, we performed intracellular staining overnight, followed by triplicate washing and the addition of appropriate secondary antibodies. The following MGMT antibodies were used: anti-MGMT (1:200; Cell Signaling Technology, Danvers, MA). In addition, as secondary antibodies we used anti-rabbit immunoglobulin G–fluorescein isothiocyanate (1:500; Thermo Fisher Scientific, Waltham, MA, USA) and anti-mouse immunoglobulin G–PB (1:500; Thermo Fisher Scientific). Samples were run on a BD LSRFortessa 6-Laser fluorescence-activated cell sorting analyzer and were analyzed using FlowJo software (TreeStar, Ashland, OR). To label dead cells, 0.1 μg/ml of 7-amino-actinomycin D (BD Pharmingen, San Jose, CA) was applied for 10 minutes. Staining was quantified using flow cytometry (BD LSRII-Blue). Data analysis was performed on FlowJo software.

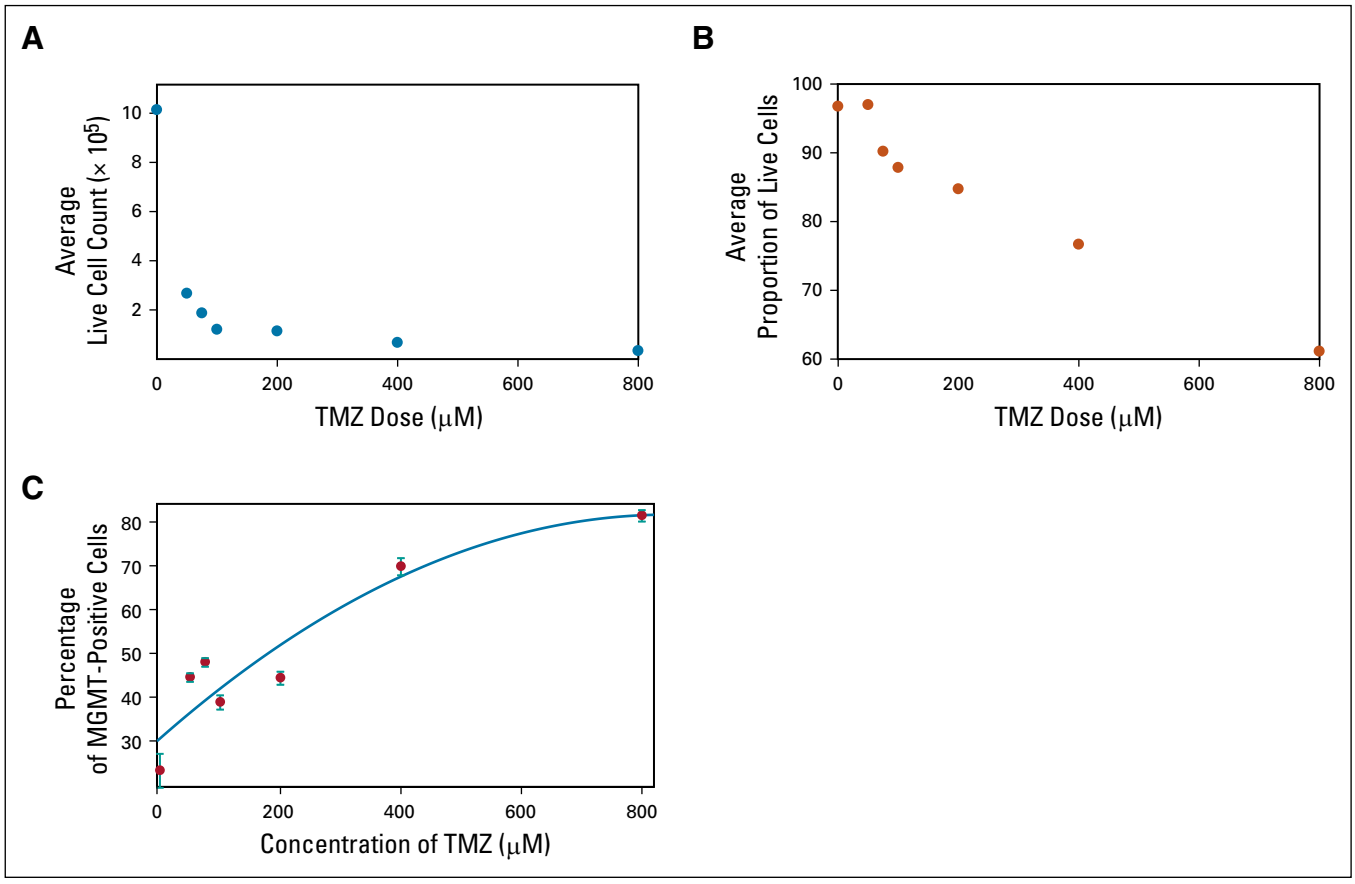

FIG 2. (A) Plot shows the average live cell counts collected after 8 days of exposure to temozolomide (TMZ) as a function of the concentration of TMZ exposure (in micromolar). (B) Plot shows the mean proportion of live cells of the total cells (live and dead cells) after 8 days of exposure as a function of the concentration of the TMZ dose (in micromolar). (C) Plot shows the percentage of cells expressing MGMT after 8 days of exposure to various concentrations of TMZ (in micromolar), assessed using patient-derived xenograft experiments. Red dots in the plot denote average percentages of MGMT-positive cells, and the error bars indicate standard deviation. The nonlinear least squares regression curve is $P^+ = 17.22 \log(0.142\ C)$, $R^2 = 0.965$, where P^+ is the percentage of cells expressing MGMT and C denotes the concentration of TMZ.

Clinical Data

Clinical data were also collected from a group of 21 adult patients (average age, 54.37 ± 13.25 years; female, n = 8; male, n = 13) with primary glioblastoma who received the standard protocol described in Stupp et al.[1] Tumor radius size was collected from each patient at initial detection and at recurrence. These data are summarized in Figure 3A. Tumor growth in the absence of treatment was also tracked, which resulted in net growth rate estimates for each patient, summarized in Figure 3C. Using patient data and a reaction-diffusion model described in Corwin et al,[41] we obtained an average net growth rate estimate of $\lambda = 0.0897$ per cell per day before treatment. Patient data that describe tumor radius size after surgery is displayed in Figure 3C. Clinical data are used in the Data Supplement to characterize the intrinsic cellular growth rates in the absence of treatment and tumor size at detection and after surgery within the model, assuming a roughly spherical tumor.

We note that WHO has recently updated its classification of brain tumors to distinguish IDH1 mutant from non-IDH1 mutant glioblastomas, and that the evolutionary processes between these tumor subtypes may potentially differ. In this clinical cohort, IDH1 mutation data were only available for five patients and all were nonmutants. In light of the lack of data on IDH1 status for the remaining patients in the cohort, we have not explicitly modeled the effect of these mutations within the model; however, a model that includes IDH1 status will be the subject of future work.

RESULTS

To demonstrate the model dynamics, we first provide a single sample path simulation of the model in Figure 4A which shows the type 1 (methylated) and total population sizes during the standard treatment regimen. Figure 4B shows the distribution of recurrence times from a computational experiment with 100 Monte Carlo simulations. Mean recurrence time is 214.17 ± 2.78 days and median recurrence time is 213.8 days, which is roughly consistent with clinical data in Ogura et al,[42] who reported a median recurrence time of 191 days.

Selection Alone Does Not Explain Methylation Shift in Recurrent Tumors

Using the parameter settings obtained from the calibration described in the Data Supplement, we next examined the relative methylation percentages at diagnosis and recurrence. Figures 4C and 4D show the distribution of methylation percentages found at these times. We observe

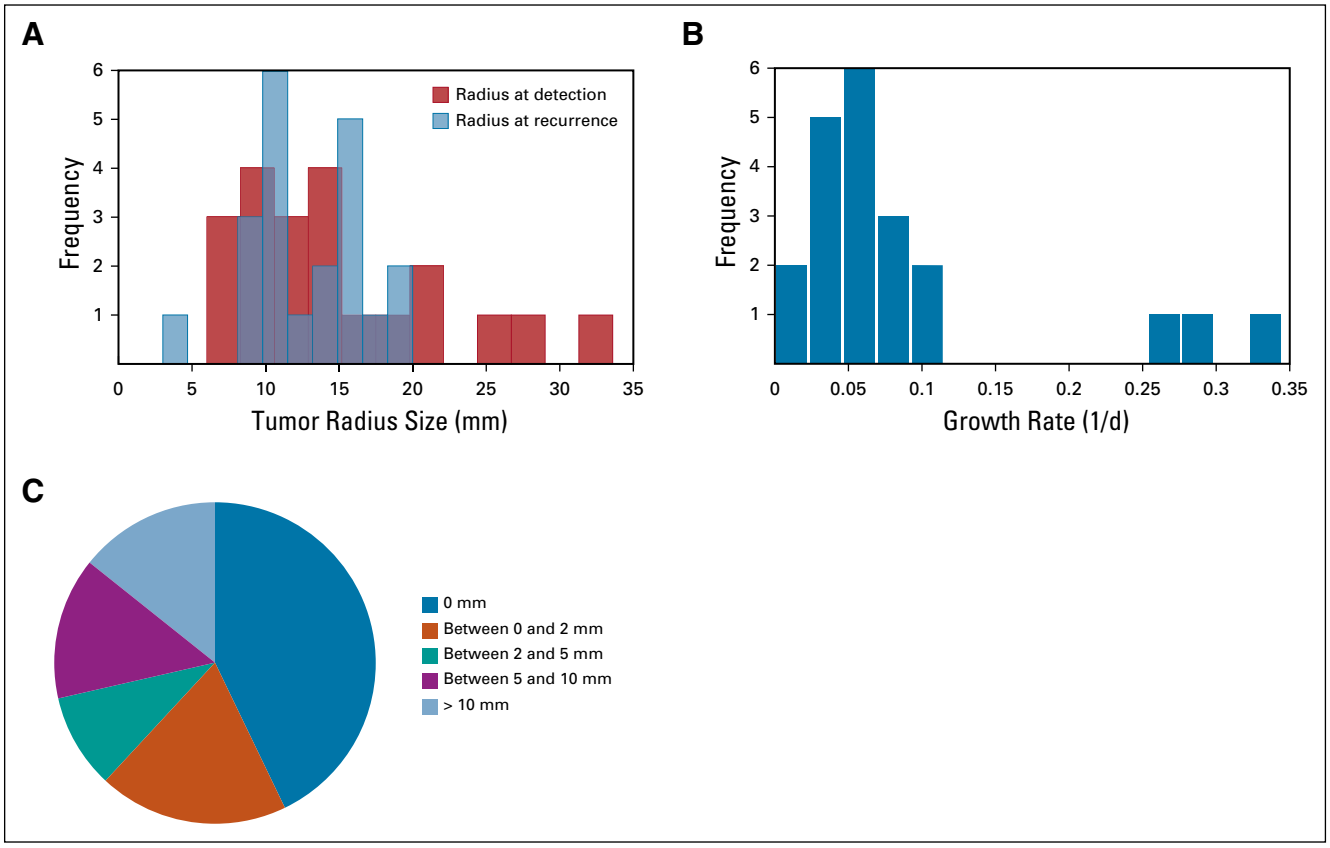

FIG 3. Clinical data from patients with glioblastoma multiforme undergoing standard regimen (n = 21). (A-C) Histograms of tumor radius at detection and recurrent tumor radius (in millimeters; A), overall net growth rate (1/d) before treatment (B), and a pie chart depicting the radius of tumor remaining after surgery (in millimeters; C).

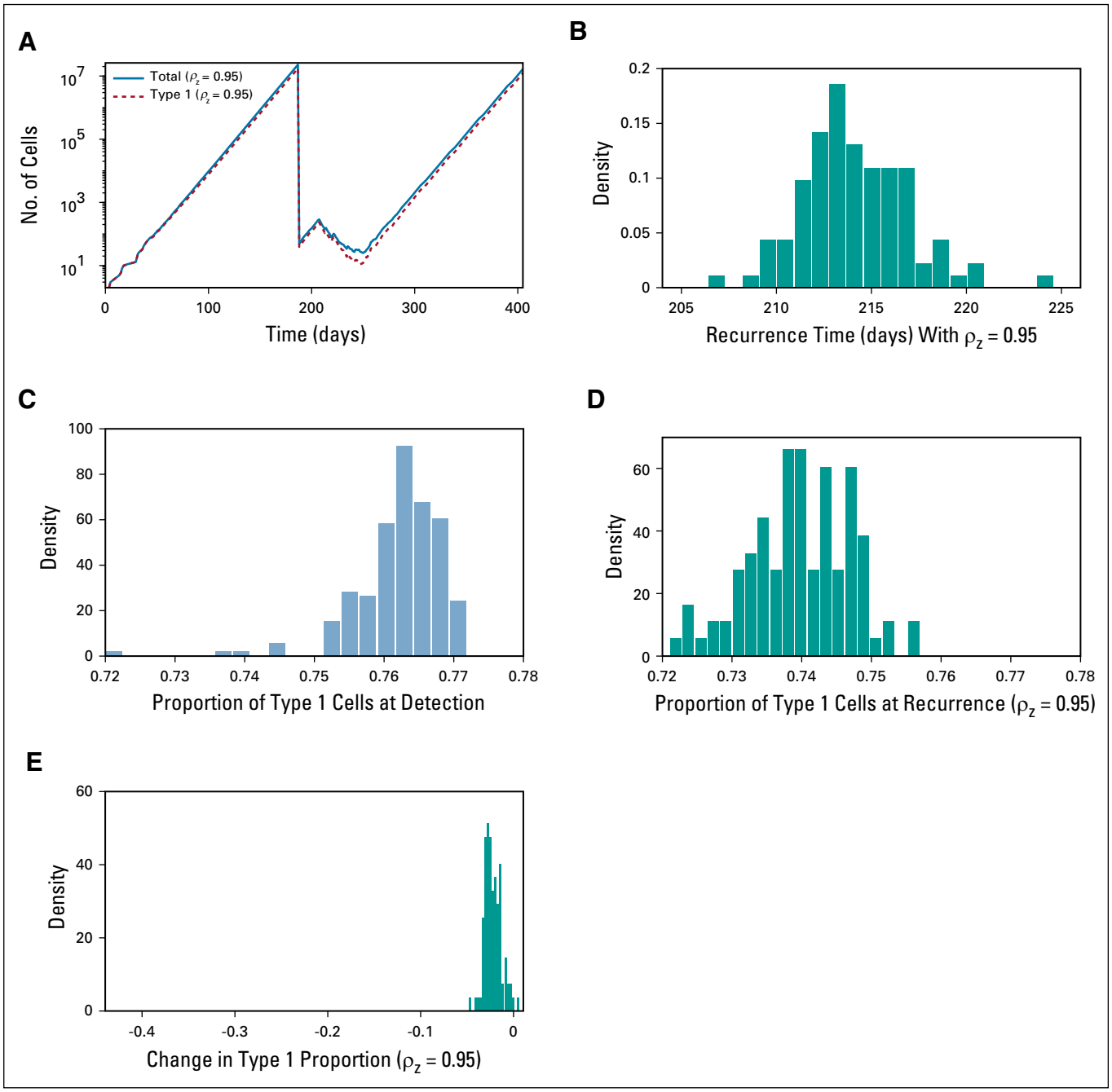

FIG 4. Simulation results with no temozolomide impact on methylation rates. (A-E) Plots of one sample path simulation of the model (A), distribution of recurrence times in a computational experiment with 100 samples (B), distribution of methylation percentage at the time of detection (C), distribution of methylation percentage at the time of recurrence (D), and distribution of change in methylation percentage between detection and recurrence (E). All parameters are set as described in the Data Supplement.

that the average proportions of methylated (type 1) cells to total cells at recurrence and diagnosis are roughly the same. Distribution of the change in methylation percentage between detection and recurrence is depicted in Figure 4E. The slight reduction in overall methylation percentage suggests that evolutionary selection alone cannot account for the significant reduction in methylation observed in the clinical studies described in Introduction.

TMZ Inhibition of Maintenance Methylation Results in Downward Methylation Shift

We next investigated the hypothesis that TMZ actively affects cellular methylation processes, driving the methylation downshift in recurrent tumors. In particular, we investigated the possibility that TMZ may decrease the amount of time spent in the type 1 (methylated) state and increase time spent in type 2/type 3 states. This may result

from a decrease in either the de novo methylation probability, ν, or the maintenance methylation probability, ρ. Of note, for this investigation, the parameters ν, ρ will deviate from their baseline values only during TMZ treatment periods; we denote the parameters during TMZ treatment as ν_z, ρ_z.

To investigate the effects of changing the de novo methylation probability, ν_z, in the presence of TMZ, we first note that the lowest possible value of ν_z is 0, which represents no de novo methylation events. When we let $\nu_z = 0$, we observe a modest decrease in the expected methylation percentage between detection and recurrence, changing by approximately 7%. Figures 5A and 5B show the distribution of methylation percentages at the time of recurrence and the distribution of change in methylation percentage between detection and recurrence, respectively, when $\nu_z = 0$. Thus, a significant drop in methylation percentage after TMZ treatment cannot be attributed to an inhibitory impact on de novo methylation.

We next investigated the impact of decreasing the probability of maintenance methylation, ρ_z, during chemotherapy. Figure 5C displays the type 1 frequency at the time of recurrence when $\rho_z = 0.5$, reduced from the baseline value of $\rho = 0.95$, and Figure 5D shows the change in methylation percentage between detection and recurrence. We observe that there is a much more significant decrease in methylation in this case than when TMZ does not affect methylation rates—compare Figures 5D and 4E). Figure 5E shows the expected proportion of type 1 cells at recurrence, as a function of ρ_z. For smaller values of ρ_z, the proportion of type 1 cells after treatment decreases substantially from a mean methylation percentage of 0.762 at detection. Thus, TMZ inhibition of maintenance methylation, but not de novo methylation, can explain the clinically observed downward shift in methylation. To account for possible error resulting from a limited clinical sample size, in the Data Supplement we demonstrate that this claim is robust to model parameter variability.

Optimization of Adjuvant TMZ Schedule to Minimize Expected Tumor Size

We next used the model to investigate the optimal number of TMZ doses during phase 3, the adjuvant chemotherapy phase, to minimize the expected tumor size after four cycles of treatment. In the standard treatment schedule, five TMZ doses of 150 to 200 mg/m^2 are administered daily at the beginning of each 28-day cycle. Let n denote the number of TMZ doses in a single 28-day cycle. We vary n to determine the number of doses and dose level that minimizes the number of total cells remaining after four adjuvant cycles. Let Z(n) denote the TMZ concentration level per dose, in milligrams per square meter, when n doses are administered per cycle. Each dose concentration is set at Z(n) = 1,000/n for varying values of n, where $0 < n < 28$, so that the cumulative TMZ dose per cycle does not exceed 1,000 mg/m^2. On the basis of our previous investigations, the maintenance methylation probability in the presence of TMZ, ρ_z, is assumed to be 0.5.

Mean calculations for each cell type, provided in the Data Supplement, are used to determine the n that minimizes the expected tumor size after four cycles. Figures 6A and 6B show the mean tumor size, number of fully methylated cells (type 1), and cells that are not fully methylated (type 2 and type 3) when $\rho_z = 0.5$. In this case, the optimal number of doses per cycle—that is, the number that results in the smallest mean tumor population after four cycles—is n = 6, with Z(6) = 166.67 mg/m^2. This is close to the standard administered dose during adjuvant chemotherapy, and we observe a small difference in the expected tumor size when five versus six doses are administered. Hence, our model suggests that the standard dosing schedule is a reasonable, though not optimal, protocol for highly methylated tumors at diagnosis.

We also used the model to investigate the optimal adjuvant TMZ schedule for tumors with lower methylation percentages at diagnosis. To this end, we first identified the combination of birth rates ($b_1 = 0.0569$ day^{-1} and $b_2 = 0.1276$ day^{-1}) that satisfied the net growth rate constraint and led to 30% methylation at detection. Figures 6C and 6D display plots of the mean number of total, fully methylated (type 1), and nonmethylated (type 2 and type 3) cells as functions of the number of doses per cycle. We observe that the tumor is dominated by nonmethylated cells for all n, and the large population of TMZ-resistant cells makes a large number of TMZ doses less effective. In addition, whereas n = 3 is the optimal dose number in this case, it is not significantly more beneficial than no adjuvant TMZ treatment. Such behavior is consistent with clinical observations. The study by Hervouet et al[2] found that unmethylated tumors that were treated with radiotherapy and the standard TMZ regimen had a median overall survival of 12.7 months versus a median overall survival of 11.8 months for those who received only radiotherapy. Thus, our model suggests that tumors with low levels of methylation at diagnosis may be better served by alternative therapies, such as O6-benzylguanine discussed in Adair et al,[43] that can be used in combination with TMZ to counter the effect of TMZ on the methylation process.

DISCUSSION

In this work, we developed a mathematical model that integrates a mechanistic description of MGMT promoter methylation/demethylation with the evolutionary dynamics of GBM tumor progression during standard treatment. We investigated several possible causes for the clinically observed drop in methylation percentage between primary and recurrent tumor stages. Our results indicate that this clinically observed methylation reduction cannot be explained by evolutionary selection, which suggests that TMZ may play an active role in altering methylation

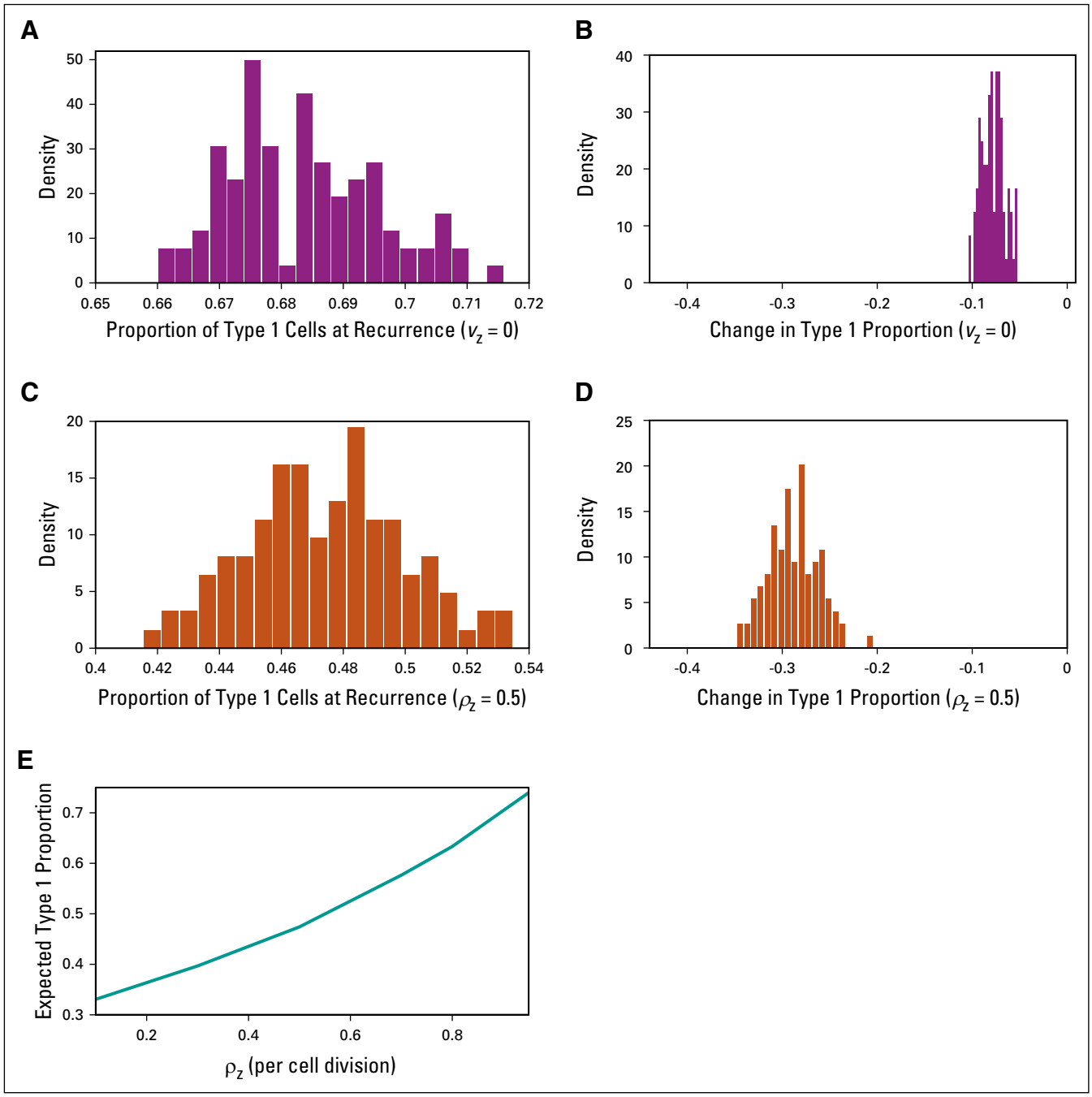

FIG 5. Simulation results with temozolomide inhibition of methylation rates. (A-E) Plots of the distribution of methylation percentage at the time of recurrence when $v_z = 0$ (A), distribution of change in methylation percentage between detection and recurrence when $v_z = 0$ (B), distribution of methylation percentage at the time of recurrence when $\rho_z = 0.5$ (C), distribution of change in methylation percentage between detection and recurrence when $\rho_z = 0.5$ (D), and expected proportion of type 1 cells at recurrence under the standard treatment schedule as a function of the maintenance methylation probability, ρ_z (E). Nonvarying parameters are set to the baseline values described in the Data Supplement.

processes. Investigating this further, we found that TMZ inhibition of the maintenance methylation results in a sizable reduction in expected methylation percentage at recurrence, which is consistent with clinical results.

The precise mechanism by which TMZ may contribute to MGMT demethylation is unclear, but experimental studies suggest that this may involve the activation of the protein kinase C (PKC) signaling pathway. In Boldogh et al,[44] it was demonstrated that alkylating drugs similar to TMZ led to an increase in MGMT expression and PKC activity. In Lavoie et al,[45] the authors discovered that a number of PKC isoforms induce the attachment of a phosphoryl group to DNMT1. Additional testing on the specific isoform PKCζ demonstrated that cells with a high expression of both PKCζ

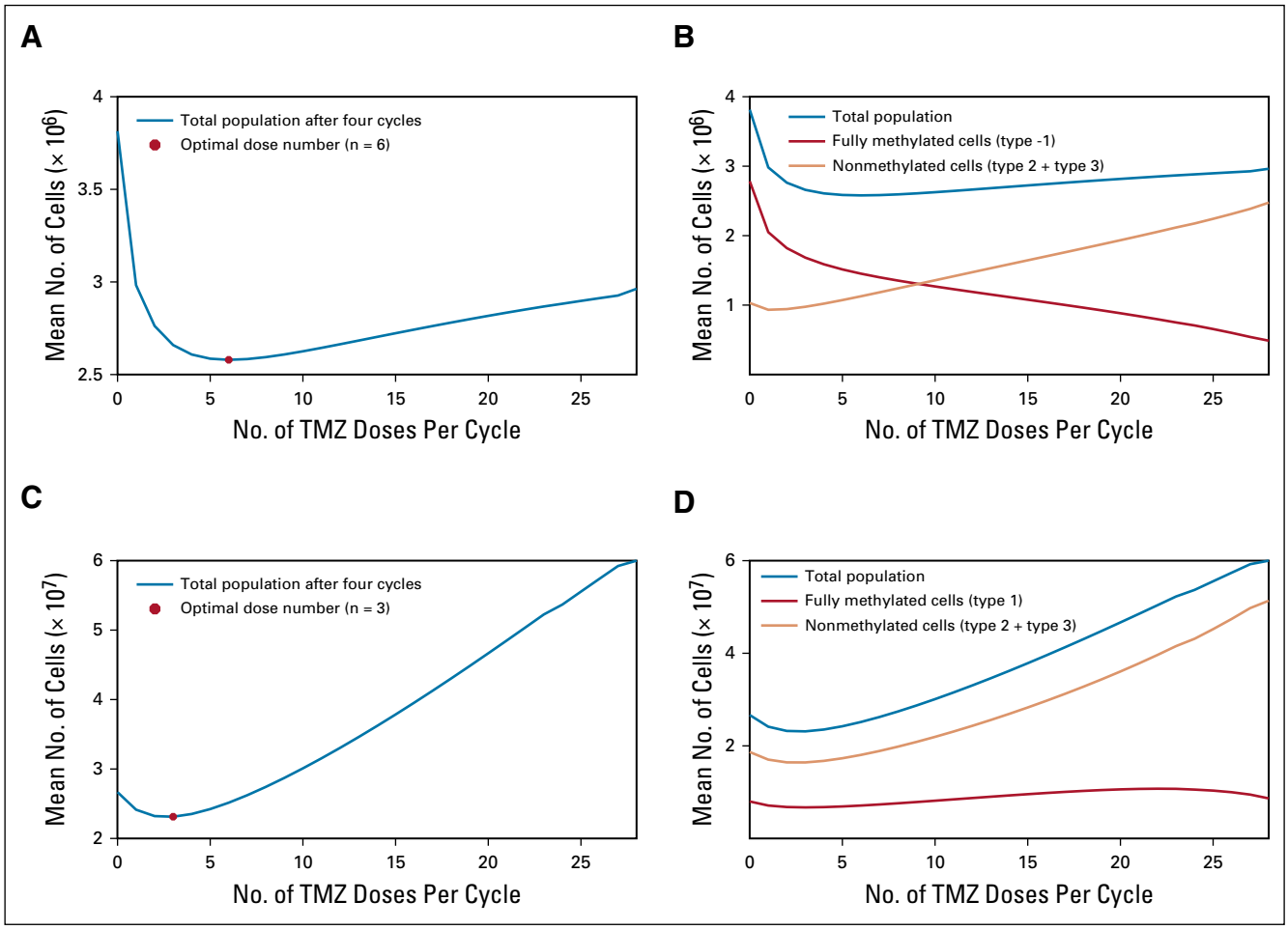

FIG 6. Adjuvant temozolomide optimization comparison between tumors with high and low levels of methylation at diagnosis. (A-D) Plots of the mean tumor population size (A) and the mean total, type 1, and type 2/type 3 cell population size when $\rho_z = 0.5$ (B), as well as the mean tumor population size (C) and the mean total, type 1, and type 2/type 3 cell population size (D) when the expected methylation proportion at diagnosis is 0.3. Mean cell populations are calculated after four adjuvant chemotherapy cycles as a function of the number of doses in one cycle during phase 3. We use the standard set of parameters. In panels A and C, we also plot the optimal number of TMZ doses (n = 6 and n = 3, respectively) and the corresponding tumor size in red.

and DNMT1 exhibited a significant reduction in methylation. This was not the case in cells with a high expression of PKCζ or DNMT1 alone. This suggests that methylation reduction results from the phosphorylation of DNMT1, driven by PKCζ. Another study in Ichimura et al[46] confirms that the phosphorylation of DNMT1 is associated with hypomethylation of gene promoters. Hence, experimental studies suggest that TMZ may contribute to MGMT demethylation by activating the PKC signaling pathway in GBM cells, which leads to the phosphorylation of DNMT1, thereby inhibiting maintenance methylation within the affected cells as our model suggests. It also may be the case that TMZ affects the activity of proteins TET1 and TET2, which have been shown to implicitly inhibit DNMT1 activity.[32,33]

Incorporating the proposed TMZ effect, we used the model to find the optimal number of TMZ doses administered during adjuvant chemotherapy. The number of daily TMZ doses administered during each cycle was varied while maintaining the same cumulative dose per cycle to determine the dose number that minimizes the mean tumor population after four adjuvant cycles. We determined an optimal TMZ dosing schedule of six daily doses of 166.67 mg/m^2, followed by 22 days off. The standard schedule of five daily doses per cycle is nearly optimal, resulting in a slightly larger mean tumor size after four cycles. We also investigated the optimal adjuvant chemotherapy schedule for a tumor with a low methylation percentage at diagnosis. Receiving three larger doses of TMZ is optimal in this case, but does not provide a significant benefit over the absence of any adjuvant TMZ treatment. This observation is consistent with clinical results that compare the benefit of both radiotherapy and chemotherapy with radiotherapy alone for unmethylated primary tumors. Therefore, our model suggests that for primarily unmethylated tumors it may be more beneficial to administer, in combination with TMZ,

a therapy that can stimulate MGMT methylation within the tumor. We would like to explore in the future whether upregulating de novo methylation counteracts the TMZ-mediated reduction in MGMT methylation.

A limitation of our model is that we assume a roughly spherical tumor—not incorporating the diffuse nature of GBM—and we do not distinguish between tumors located in different places in the brain. We also assume that all hemimethylated and unmethylated GBM cells behave with the same intrinsic growth rates and that MGMT methylation status does not affect radiosensitivity. Of note, a few studies have suggested that there may be a phenomenon of MGMT depletion after extended exposure to TMZ in an attempt to explain observed differences in dose-dense TMZ treatment and the standard TMZ regimen.[47,48] If this phenomenon occurs, it would make TMZ more effective in tumors with low methylation levels; however, other studies have found no conclusive differences in dose-dense TMZ regimens and the standard TMZ regimen for all GBM.[49,50] Thus, we did not incorporate a mechanism for MGMT depletion in our model. In future work, we plan to investigate the hypothesis that the oncogenic IDH1 mutation drives increased methylation in gliomas, particularly in the context of secondary GBM.[46,51]

AFFILIATIONS

[1]University of Minnesota Twin Cities, Minneapolis, MN
[2]Mayo Clinic, Phoenix, AZ
[3]Northwestern University Feinberg School of Medicine, Chicago, IL
[4]City of Hope National Medical Center, Duarte, CA

CORRESPONDING AUTHOR

Jasmine Foo, MD, University of Minnesota Twin Cities, 206 Church St SE, Minneapolis, MN 55455; Twitter: @UMNresearch; e-mail: jyfoo@umn.edu.

SUPPORT

Supported by National Science Foundation Grant No. DMS-1349724 (K.S. and J.F.), National Science Foundation Grant No. CMMI-1362236 (K.S. and K.L.), National Cancer Institute Grant No. P30-CA033572 (R.C.R.), National Institute of Neurologic Disorders and Stroke Grant No. 1R01-NS096376 (A.U.A.), and American Cancer Society Grant No. RSG-16-034-01-DDC (A.U.A.).

AUTHOR CONTRIBUTIONS

Conception and design: Katie Storey, Kevin Leder, Andrea Hawkins-Daarud, Kristin Swanson, Russell C. Rockne, Jasmine Foo
Financial support: Kevin Leder, Atique U. Ahmed, Jasmine Foo
Provision of study materials or patients: Kristin Swanson
Data analysis and interpretation: Katie Storey, Kevin Leder, Kristin Swanson, Atique U. Ahmed, Jasmine Foo
Manuscript writing: All authors
Final approval of manuscript: All authors
Accountable for all aspects of the work: All authors

AUTHORS' DISCLOSURES OF POTENTIAL CONFLICTS OF INTEREST AND DATA AVAILABILITY STATEMENT

The following represents disclosure information provided by authors of this manuscript. All relationships are considered compensated. Relationships are self-held unless noted. I = Immediate Family Member, Inst = My Institution. Relationships may not relate to the subject matter of this manuscript. For more information about ASCO's conflict of interest policy, please refer to www.asco.org/rwc or ascopubs.org/jco/site/ifc.

No potential conflicts of interest were reported.

ACKNOWLEDGMENT

The authors thank C. David James, MD, for providing all the patient-derived xenografts lines. The content is solely the responsibility of the authors and does not necessarily represent the official views of the funding organizations.

REFERENCES

1. Stupp R, Mason WP, van den Bent MJ, et al: Radiotherapy plus concomitant and adjuvant temozolomide for glioblastoma. N Engl J Med 352:987-996, 2005
2. Hervouet E, Lalier L, Debien E, et al: Disruption of Dnmt1/PCNA/UHRF1 interactions promotes tumorigenesis from human and mice glial cells. PLoS One 5:e11333, 2010
3. Hegi ME, Diserens AC, Gorlia T, et al: MGMT gene silencing and benefit from temozolomide in glioblastoma. N Engl J Med 352:997-1003, 2005
4. Zhang J, Stevens MF, Bradshaw TD: Temozolomide: Mechanisms of action, repair and resistance. Curr Mol Pharmacol 5:102-114, 2012
5. Kitange GJ, Carlson BL, Schroeder MA, et al: Induction of MGMT expression is associated with temozolomide resistance in glioblastoma xenografts. Neuro-oncol 11:281-291, 2009
6. Brandes AA, Franceschi E, Tosoni A, et al: O^6-methylguanine DNA-methyltransferase methylation status can change between first surgery for newly diagnosed glioblastoma and second surgery for recurrence: Clinical implications. Neuro-oncol 12:283-288, 2010
7. Suzuki T, Nakada M, Yoshida Y, et al: The correlation between promoter methylation status and the expression level of O^6-methylguanine-DNA methyltransferase in recurrent glioma. Jpn J Clin Oncol 41:190-196, 2011
8. Jung TY, Jung S, Moon KS, et al: Changes of the O^6-methylguanine-DNA methyltransferase promoter methylation and MGMT protein expression after adjuvant treatment in glioblastoma. Oncol Rep 23:1269-1276, 2010
9. Christmann M, Nagel G, Horn S, et al: MGMT activity, promoter methylation and immunohistochemistry of pretreatment and recurrent malignant gliomas: A comparative study on astrocytoma and glioblastoma. Int J Cancer 127:2106-2118, 2010
10. Brown R, Curry E, Magnani L, et al: Poised epigenetic states and acquired drug resistance in cancer. Nat Rev Cancer 14:747-753, 2014
11. Levin VA, Patlak CS, Landahl HD: Heuristic modeling of drug delivery to malignant brain tumors. J Pharmacokinet Biopharm 8:257-296, 1980
12. Stamatakos GS, Antipas VP, Uzunoglu NK: A spatiotemporal, patient individualized simulation model of solid tumor response to chemotherapy in vivo: The paradigm of glioblastoma multiforme treated by temozolomide. IEEE Trans Biomed Eng 53:1467-1477, 2006
13. Böttcher MA, Held-Feindt J, Synowitz M, et al: Modeling treatment-dependent glioma growth including a dormant tumor cell subpopulation. BMC Cancer 18:376, 2018

14. Franken NA, Hovingh S, Rodermond H, et al: Radiosensitization with chemotherapeutic agents and hyperthermia: Effects on linear-quadratic parameters of radiation cell survival curves. J Cancer Sci Ther S5:002, 2011
15. Brenner DJ: The linear-quadratic model is an appropriate methodology for determining isoeffective doses at large doses per fraction. Semin Radiat Oncol 18:234-239, 2008
16. Zaider M, Minerbo GN: Tumour control probability: A formulation applicable to any temporal protocol of dose delivery. Phys Med Biol 45:279-293, 2000
17. Badri H, Pitter K, Holland EC, et al: Optimization of radiation dosing schedules for proneural glioblastoma. J Math Biol 72:1301-1336, 2016
18. Powathil G, Kohandel M, Sivaloganathan S, et al: Mathematical modeling of brain tumors: Effects of radiotherapy and chemotherapy. Phys Med Biol 52:3291-3306, 2007
19. Rockne R, Rockhill JK, Mrugala M, et al: Predicting the efficacy of radiotherapy in individual glioblastoma patients in vivo: A mathematical modeling approach. Phys Med Biol 55:3271-3285, 2010
20. Esteller M, Hamilton SR, Burger PC, et al: Inactivation of the DNA repair gene O^6-methylguanine-DNA methyltransferase by promoter hypermethylation is a common event in primary human neoplasia. Cancer Res 59:793-797, 1999
21. Håvik AB, Brandal P, Honne H, et al: MGMT promoter methylation in gliomas-assessment by pyrosequencing and quantitative methylation-specific PCR. J Transl Med 10:36, 2012
22. Yatabe Y, Tavaré S, Shibata D: Investigating stem cells in human colon by using methylation patterns. Proc Natl Acad Sci USA 98:10839-10844, 2001
23. Otto SP, Walbot V: DNA methylation in eukaryotes: Kinetics of demethylation and de novo methylation during the life cycle. Genetics 124:429-437, 1990
24. Gilbert MR, Wang M, Aldape KD, et al: Dose-dense temozolomide for newly diagnosed glioblastoma: A randomized phase III clinical trial. J Clin Oncol 31:4085-4091, 2013
25. Sontag LB, Lorincz MC, Georg Luebeck E: Dynamics, stability and inheritance of somatic DNA methylation imprints. J Theor Biol 242:890-899, 2006
26. Pfeifer GP, Steigerwald SD, Hansen RS, et al: Polymerase chain reaction-aided genomic sequencing of an X chromosome-linked CpG island: Methylation patterns suggest clonal inheritance, CpG site autonomy, and an explanation of activity state stability. Proc Natl Acad Sci USA 87:8252-8256, 1990
27. Kim GD, Ni J, Kelesoglu N, et al: Co-operation and communication between the human maintenance and de novo DNA (cytosine-5) methyltransferases. EMBO J 21:4183-4195, 2002
28. Chen T, Ueda Y, Dodge J.E., et al: Establishment and maintenance of genomic methylation patterns in mouse embryonic stem cells by Dnmt3a and Dnmt3b. Mol Cell Biol 23:5594-5605, 2003
29. Vilkaitis G, Suetake I, Klimasauskas S, et al: Processive methylation of hemimethylated CpG sites by mouse Dnmt1 DNA methyltransferase. J Biol Chem 280:64-72, 2005
30. Tahiliani M, Koh KP, Shen Y, et al: Conversion of 5-methylcytosine to 5-hydroxymethylcytosine in mammalian DNA by MLL partner TET1. Science 324:930-935, 2009
31. Williams K, Christensen J, Pedersen MT, et al: TET1 and hydroxymethylcytosine in transcription and DNA methylation fidelity. Nature 473:343-348, 2011
32. Hatzikirou H, Deutsch A, Schaller C, et al: Mathematical modelling of glioblastoma tumour development: a review. Math Mod Methods Appl Sci 24:1779-1794, 2005
33. Ji D, Lin K, Song J, et al: Effects of Tet-induced oxidation products of 5-methylcytosine on Dnmt1- and DNMT3a-mediated cytosine methylation. Mol Biosyst 10:1749-1752, 2014
34. Athreya KB, Ney PE: Branching Processes. New York, NY, Springer, 1972
35. Genereux DP, Miner BE, Bergstrom CT, et al: A population-epigenetic model to infer site-specific methylation rates from double-stranded DNA methylation patterns. Proc Natl Acad Sci USA 102:5802-5807, 2005
36. Carlson BL, Grogan PT, Mladek AC, et al: Radiosensitizing effects of temozolomide observed in vivo only in a subset of O^6-methylguanine-DNA methyltransferase methylated glioblastoma multiforme xenografts. Int J Radiat Oncol Biol Phys 75:212-219, 2009
37. Fowler JF: The linear-quadratic formula and progress in fractionated radiotherapy. Br J Radiol 62:679-694, 1989
38. Beier D, Röhrl S, Pillai DR, et al: Temozolomide preferentially depletes cancer stem cells in glioblastoma. Cancer Res 68:5706-5715, 2008
39. Rosso L, Brock CS, Gallo JM, et al: A new model for prediction of drug distribution in tumor and normal tissues: Pharmacokinetics of temozolomide in glioma patients. Cancer Res 69:120-127, 2009
40. Ostermann S, Csajka C, Buclin T, et al: Plasma and cerebrospinal fluid population pharmacokinetics of temozolomide in malignant glioma patients. Clin Cancer Res 10:3728-3736, 2004
41. Corwin D, Holdsworth C, Rockne RC, et al: Toward patient-specific, biologically optimized radiation therapy plans for the treatment of glioblastoma. PLoS One 8:e79115, 2013
42. Ogura K, Mizowaki T, Arakawa Y, et al: Initial and cumulative recurrence patterns of glioblastoma after temozolomide-based chemoradiotherapy and salvage treatment: A retrospective cohort study in a single institution. Radiat Oncol 8:97, 2013
43. Adair JE, Johnston SK, Mrugala MM, et al: Gene therapy enhances chemotherapy tolerance and efficacy in glioblastoma patients. J Clin Invest 124:4082-4092, 2014
44. Boldogh I, Ramana CV, Chen Z, et al: Regulation of expression of the DNA repair gene O^6-methylguanine-DNA methyltransferase via protein kinase C-mediated signaling. Cancer Res 58:3950-3956, 1998
45. Lavoie G, Estève PO, Laulan NB, et al: PKC isoforms interact with and phosphorylate DNMT1. BMC Biol 9:31, 2011
46. Ichimura K, Pearson DM, Kocialkowski S, et al: IDH1 mutations are present in the majority of common adult gliomas but rare in primary glioblastomas. Neuro-oncol 11:341-347, 2009
47. Brandes AA, Tosoni A, Cavallo G, et al: Temozolomide 3 weeks on and 1 week off as first-line therapy for recurrent glioblastoma: Phase II study from Gruppo Italiano Cooperativo di Neuro-Oncologia (GICNO). Br J Cancer 95:1155-1160, 2006
48. Wick W, Platten M, Weller M: New (alternative) temozolomide regimens for the treatment of glioma. Neuro-oncol 11:69-79, 2009
49. Mehta MP, Wang M, Aldape K, et al: RTOG 0525: Exploratory subset analysis from a randomized phase III trial comparing standard adjuvant temozolomide with a dose-dense schedule for glioblastoma. Int J Rad Oncol Biol Phys 81:S128-S129, 2011
50. Hashimoto H, Liu Y, Upadhyay AK, et al: Recognition and potential mechanisms for replication and erasure of cytosine hydroxymethylation. Nucleic Acids Res 40:4841-4849, 2012
51. Molenaar RJ, Verbaan D, Lamba S, et al: The combination of IDH1 mutations and MGMT methylation status predicts survival in glioblastoma better than either IDH1 or MGMT alone. Neuro-oncol 16:1263-1273, 2014

